

# Multiple-photon resolving fiber-loop detector

J. Řeháček and Z. Hradil

*Department of Optics, Palacky University, 17. listopadu 50, 772 00 Olomouc, Czech Republic*

O. Haderka, J. Peřina Jr., and M. Hamar

*Joint Laboratory of Palacky University and the Institute of Physics of the Czech Academy of Sciences, 17. listopadu 50, 772 00 Olomouc, Czech Republic*

We show first reconstructions of the photon-number distribution obtained with a multi-channel fiber-loop detector. Apart from analyzing the statistics of light pulses this device can serve as a sophisticated post-selection device for experiments in quantum optics and quantum information. We quantify its efficiency by means of the Fisher information and compare it to the efficiency of the ideal photodetector.

A major drawback of common detectors of weak light fields is their lack of photon-number resolution. Due to the nonlinear character of amplifying process the response of such detectors is not sensitive to the strength of the input signal. The only two detection events in such a case are “click” and “no click” that correspond to the presence or absence of the signal. A device capable of photon-number resolution would contribute both to fundamental research in quantum optics and to implementation of quantum communication and information protocols. While such devices were recently indeed constructed [1, 2, 3, 4, 5, 6], they require operation under extreme conditions at present and therefore did not become a common laboratory tool yet. Also, their photon-number resolution is still limited to only few photons.

Another way of circumventing this problem is splitting the input pulse using a multiport device followed by an array of conventional binary detectors as was proposed in [7, 8]. In the ideal case of many output ports the input pulse gets perfectly split and each photon is detected separately. However reasonable performance of such device would require a very large number of beamsplitters and detectors which would result in a bulky and costly detection device. It has been suggested [9] to replace the complicated multiport device by a fiber loop and a single photodetector, see Fig. 1. After each round-trip part of the incoming pulse gets transmitted to a conventional binary detector. This results in a time resolved series of detections, each of them corresponding to a different out-

put port of the multiport device. Such a multiple photon resolving device has recently been built in our laboratory [10]. The variable ratio coupler inserted at the entrance to the fiber-loop delay line, see Fig. 1, is used to adjust the transmission probabilities of the output channels to a certain extent and thus tweak the overall resolving power of our instrument.

The purpose of this communication is twofold. First, we will analyze the performance of the fiber-loop detector and compare it to the efficiency of the ideal photodetection device. Second, we will show how to reconstruct the photon statistics of the input pulse from the data measured at the fiber-loop detector via the maximum-likelihood principle and apply this technique to experimental data.

The fiber-loop detector is used to count photons contained in the input pulse in an indirect way. Therefore it is natural to relate its performance to that of the “text-book photon counter”—the ideal photodetector of quantum efficiency  $\bar{\eta}$ . The concept of the equivalent efficiency is extremely useful in this context. The equivalent efficiency of the fiber-loop detector is defined to be equal to the quantum efficiency of the ideal photodetector that gives the same measurement error. This concept was used by Braunstein and Nemoto [11] to analyze another indirect photon-counting device—the homodyne detection scheme. Since their motivation was to use the homodyne detection for signaling they chose the mutual information as their measure of the measurement accuracy. Our motivation is different. We are rather interested in the analysis of the input light statistics. Let  $\rho_n$  be the true photon-number distribution (i.e. the diagonal elements of the density matrix) of the input pulse. After  $N$  identically prepared pulses have been detected we can make an estimate of the photon number distribution  $\bar{\rho}_n$ . Due to the finite measurement time and the presence of noise it will usually differ from the true distribution. We will take the mean quadratic distance  $d = \sum_n (\rho_n - \bar{\rho}_n)^2$  between  $\rho_n$  and  $\bar{\rho}_n$  as our measure of the estimation error. Let us note that for density matrices diagonal in the Fock basis this distance equals the Hilbert-Schmidt distance between the true and estimated states. Its reciprocal divided by  $N$ ,  $I = 1/(dN)$ , quantifies the information

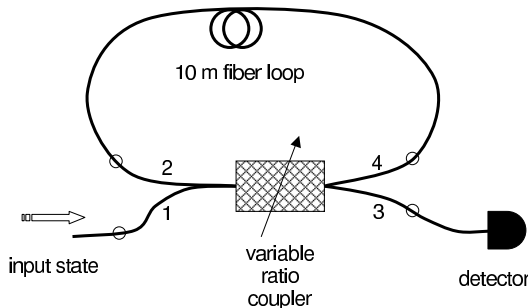


FIG. 1: Fiber-loop detector

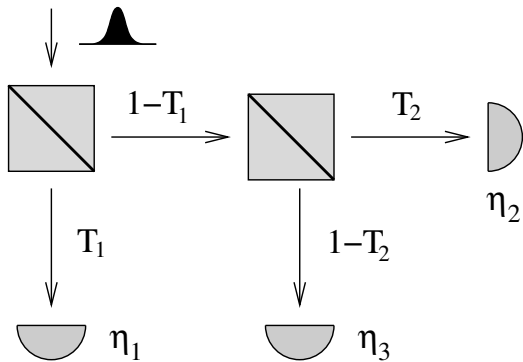


FIG. 2: Substituting scheme of the fiber-loop detector with three output channels

about the input pulse gained from the measurement per pulse. Naturally, this distance depends not only on the measurement device but also on the chosen estimation strategy. Let us calculate the error of the optimal estimation: It is well known that no matter how clever estimation procedure is adopted, its error cannot be smaller than the Cramér-Rao bound [12, 13]. This bound applied to  $I$  implies that

$$I = \left[ N \sum_n (\Delta \rho_n)^2 \right]^{-1} \leq (N \text{Tr} \mathbf{F}^{-1})^{-1}, \quad (1)$$

where  $F$  is the Fisher information matrix,

$$F_{kl} = \left\langle \frac{\partial}{\partial \rho_k} \log P(\mathbf{n}|\rho) \frac{\partial}{\partial \rho_l} \log P(\mathbf{n}|\rho) \right\rangle_{\mathbf{n}}, \quad (2)$$

and  $P(\mathbf{n}|\rho)$  is the conditional probability of detecting the outcome  $\mathbf{n}$  provided the true statistics of the input pulse is  $\rho$ . The averaging is done over the all possible outcomes  $\mathbf{n}$  of the measurement. The probability  $P(\mathbf{n}|\rho)$  completely describes the measurement apparatus. Provided the individual detection events are independent,  $P(\mathbf{n}|\rho)$  is a multinomial distribution,

$$P(\mathbf{n}|\rho) \propto \prod p_n^{N f_n}. \quad (3)$$

Here  $p_n$  is the probability that the input pulse gives rise to a detection in a particular channel  $n$ . The Fisher information matrix then simplifies to

$$F_{kl} = \frac{1}{N} \sum_n \frac{1}{p_n} \frac{\partial p_n}{\partial \rho_k} \frac{\partial p_n}{\partial \rho_l}, \quad (4)$$

In the case of the ideal detector of efficiency  $\tilde{\eta}$  the independent outcomes are just the different counted numbers of photons and the corresponding probabilities are given by the well-known Bernoulli distribution,

$$p_n = \sum_{m \geq n} \binom{m}{n} \tilde{\eta}^n (1 - \tilde{\eta})^{m-n} \rho_m. \quad (5)$$

Now we will analyze the fiber-loop detector which can be thought of as a multiport device. Such a multiport, for simplicity limited to only three output channels, is shown in Fig. 2.

The simplest situation occurs when the coincidences between detections at different output channels are not registered. Then an  $s$ -channel device reduces to  $s$  independent binary detectors of generally different quantum efficiencies. As was shown in [14], such a detection scheme already yields enough information for the reconstruction. In this case the independent events are zero-detection events in the individual channels having probabilities

$$p'_j = \sum_m [1 - \eta_j]^m \rho_m. \quad (6)$$

A significant gain in accuracy of the reconstruction can be expected when all possible coincidences are taken into account. A detection event of such a complex observation is best recorded in the binary notation where “1” or “0” appearing at a certain position corresponds to a “click” or “no click,” respectively, in the given output channel. The most simple nontrivial case of such a measurement is the fiber-loop detector with only two output channels (the pulse goes round the loop only once). This is equivalent to letting the transmissivity  $T_2$  of the second beamsplitter in Fig. 2 go to unity. In this case we have four detection events. Their probabilities read

$$\begin{aligned} p_{00} &= \sum_m \rho_m [1 - \eta_1 T - \eta_2 (1 - T)]^m, \\ p_{10} &= \sum_m \rho_m [1 - \eta_2 (1 - T)]^m - p_{00}, \\ p_{01} &= \sum_m \rho_m (1 - \eta_1 T)^m - p_{00}, \\ p_{11} &= 1 - p_{00} - p_{10} - p_{01}, \end{aligned} \quad (7)$$

and  $T = T_1$ . It is clear that only weak input signals can fully be analyzed by the simple measurement (7). In the following we will assume that the input density matrix can be truncated and thus fully specified by giving its first few elements. The most simple case is a pulse containing at most two photons,

$$\rho = (1 - \rho_1 - \rho_2) |0\rangle\langle 0| + \rho_1 |1\rangle\langle 1| + \rho_2 |2\rangle\langle 2|. \quad (8)$$

A successful estimation consist in identifying the single photon and two photon contributions. Using Eqs. (4), (5), and (7) the information (1) about the state (8) yielded by the fiber-loop detector can easily be calculated. As the resulting expression is rather complicated and not suitable for discussion we will consider only the leading term of its expansions in  $\eta$ s. Even best binary detectors have  $\eta$  significantly smaller than unity guaranteeing the rapid convergence of the series. Setting

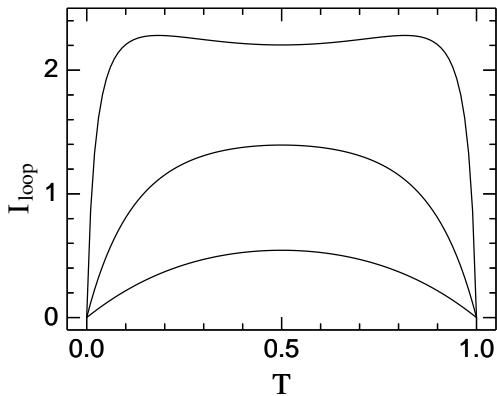


FIG. 3: Performance of the fiber-loop detector with two channels for various input states and splitting ratios. Curves from below:  $\rho_1 = 0.9$ ,  $\rho_2 = 0.1$ ;  $\rho_1 = 0.98$ ,  $\rho_2 = 0.2$ ;  $\rho_1 = 0.998$ ,  $\rho_2 = 0.002$ .

$\eta_1 = \eta_2 = \eta$  the information reads,

$$I_{\text{loop}} \approx \frac{2\tau\eta^2}{5\rho_2}, \quad \rho_2 \neq 0, \quad (9)$$

$$I_{\text{loop}} \approx \frac{2\eta}{\rho_1} + 2(1-\tau)\eta^2, \quad \rho_2 = 0, \quad (10)$$

and  $\tau = T(1-T)$ . As can be seen the information is determined by the last non-vanishing  $\rho_n$ . Naturally, states with large multi-photon contribution are more difficult to estimate. If  $\rho_2$  significantly differs from zero it is optimal to split the input pulse between the output channels equally,  $T = 1/2$ , see also Fig. (3). However for states with negligible two-photon content  $\rho_2 \approx 0$  the information exhibits a local minimum at this point, see Fig. (3). This minimum is caused by the term in Eq. (10) which is quadratic in  $\eta$  and since  $\eta$  is always significantly smaller than unity the minimum is a shallow one. In an experiment where the true state is not known,  $T = 1/2$  would be the best choice. The corresponding information gain of the ideal detector is

$$I_{\text{ideal}} \approx \frac{\bar{\eta}^2}{5\rho_2}, \quad \rho_2 \neq 0, \quad (11)$$

$$I_{\text{ideal}} \approx \frac{2\bar{\eta}}{\rho_1}, \quad \rho_2 = 0. \quad (12)$$

As can be seen, for states with negligible two-photon content the ideal and fiber-loop detectors show the same performance. This is not surprising because for single photon states there is no difference between the ideal and binary detector. However for states with significant two-photon content the information the fiber loop detector becomes inferior to the ideal one. The equivalent efficiency of the fiber-loop detector yields in the worst case can be calculated by comparing Eqs. (9) and (11),

$$\eta_{\text{eq}} \approx \eta/\sqrt{2}. \quad (13)$$

The dependence of the equivalent efficiency calculated by the exact inversion of the Fisher matrix on the quantum

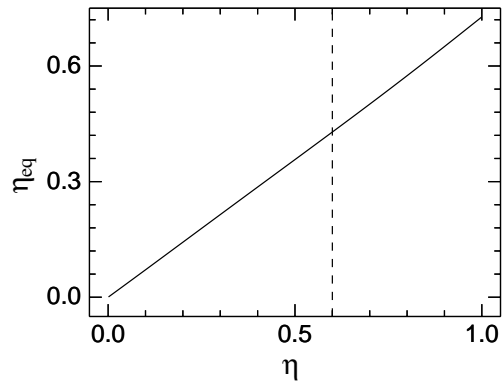


FIG. 4: Equivalent ideal detection efficiency of the fiber-loop detector with three output channels in dependence on the quantum efficiency of the binary detector used. The efficiency of standard commercial single-photon detectors is about 60% (dashed line).

efficiency of the binary detector used in the fiber-loop detector is shown in Fig. 4. As one can see Eq. (13) makes an excellent approximation. Let us close this part noting that for weak input fields the information gain of the fiber-loop and ideal detectors differ only by the factor of  $\sqrt{2}$ . Further improvement can be achieved by increasing the number of output channels. Provided the noise of the detectors can be neglected, splitting output channels into two or more new channels leads to a refinement of the probability operator measure describing the detector. Any such refinement can only increase the information gain. Such many-channel fiber-loop detectors will be discussed elsewhere.

In real experiment experimenter's control of the parameters of the fiber-loop detector is severely limited for many reasons, so it is not possible to choose the optimal configuration of the device.

Prior to its utilization the device has to be calibrated. We use coherent pulses whose statistics is known to be Poissonian for this purpose. From the probabilities of zero counts at the individual output channels the transmissions of beamsplitters in the substituting scheme are readily calculated. In the next step we calculate probabilities  $p_n$  of all possible outcomes of the experiment. We start from the probabilities of “zero-arbitrary” detection events. Such events consist of detecting nothing in given output channels while we do not care about the rest; they read

$$\tilde{p}_j = \sum_{k=0}^{\text{dim}} \left(1 - \sum_{l=0}^s \epsilon_{jl}\eta_l\right)^k \rho_k, \quad (14)$$

where  $\text{dim}$  is the chosen cutoff of the Hilbert space and  $\epsilon_{jl}$  is zero if there was an arbitrary event (denoted  $\forall$ ) detected at the  $l$ -th channel and unity if there was no detection, and  $\eta_l = \langle n_l \rangle / N$  is the detection efficiency of the  $l$ -th channel. Now the probability of having a coincidence at the first and third channels of a three-channel detector can be written in terms of the single-

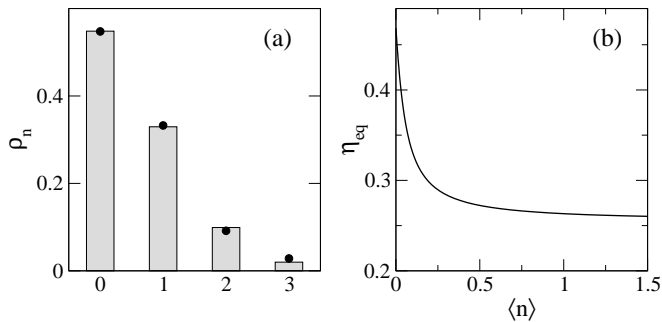


FIG. 5: (a) Reconstruction of the photon-number distribution. Black dots are the best Poissonian fit with  $\langle n \rangle \approx 0.6$  photons per pulse. (b) The calculated equivalent efficiency of the fiber-loop detector used in this experiment.

count probabilities as follows:  $p_{101} = \tilde{p}_{\vee 0 \vee} - p_{100} - p_{001} - p_{000}$ . The latter can, in turn, be expressed as  $p_{100} = \tilde{p}_{\vee 00} - p_{000}$  and  $p_{001} = \tilde{p}_{00 \vee} - p_{000}$ , respectively. The probabilities of all  $2^s$  detection events possible with an  $s$ -channel loop detector can be easily calculated using this simple recursive procedure. Having  $p_n$  determined one can proceed with the reconstruction. Notice that  $p_n$  are linear combinations of density matrix elements  $\rho_n$ ,

$$p_j = \sum_i c_{ji} \rho_i, \quad j = 1, \dots, 2^s, \quad (15)$$

$c_{ji} = \partial p_j / \partial \rho_i$  being defined by the parameters of the fiber-loop detector. The problem (15) is a typical linear and positive problem. The latter property follows from the non-negativity of  $\rho_n$ . Of course, the experimentally observed frequencies will generally differ from the theoretical probabilities,  $f_j \neq p_j$ . Because of this the problem (15) has usually no exact solution and has to be solved in the statistical sense, for example via minimization of some statistical measure of distance between  $f_j$  and  $p_j$ . We use the approach based on minimizing the Kullback-Leibler divergence (also called relative entropy)  $d = \sum_j f_j \log p_j - \sum_j f_j \log f_j$  between data and theory. The state  $\rho_n$  minimizing  $d$  is at the same time the maximum-likelihood estimator of the input state and therefore attains the Cramér-Rao bound asymptotically for large  $N$ . The minimization can be carried on e.g. via the iterative Expectation-Maximization algorithm [15, 16]:

$$\rho_k^{(n+1)} = \rho_k^{(n)} \sum_j \frac{f_j c_{jk}}{\sum_k c_{ji} \rho_i^{(n)}}. \quad (16)$$

Left panel in Fig. 5 shows the reconstruction of the photon statistics of a laser pulse containing 0.6 photons on the average. The agreement between the measured and theoretical statistics is very good. In this case only first three output channels were sufficient for the reconstruction. The equivalent efficiency of the three-channel detector calculated for Poissonian light is shown on the right in Fig. 5. We would like to emphasize that this is

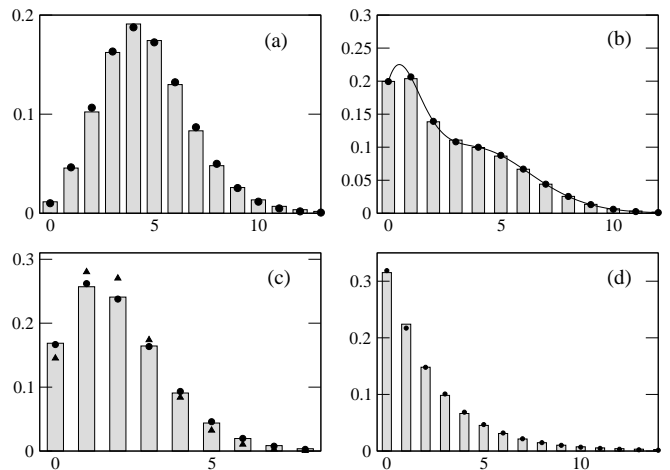


FIG. 6: Reconstructed photon-number distributions of different sources of light pulses (bars); best theoretical fits (black dots); in panel (c) best Poissonian fit is shown for comparison (triangles). Fluctuations: (a) stable amplitude,  $P(I) \propto \delta(I - I_0)$ ; (b) two-component amplitude,  $P(I) \propto \delta(I - I_1) + \delta(I - I_2)$ ; (c) uniform over the range of  $[I_3 - \delta, I_3 + \delta]$ ; (d) exponential,  $P(I) = \exp(-I/I_4)/I_4$ . Resulting statistics: (a) Poissonian; (b) composite Poissonian; (c) regularized generalized incomplete Euler gamma function; (d) Bose-Einstein. Fitted parameters:  $I_0 = 4.6$ ,  $I_1 = 0.94$ ,  $I_2 = 4.6$ ,  $I_3 = 2.0$ ,  $I_4 = 2.1$ , and  $\delta = 1.2$  photons per pulse.

the efficiency of the real experimental apparatus where a significant fraction of light is either lost inside the apparatus or not detected due to small quantum efficiency of detectors [10]. Nonetheless, in a wide range of intensities our detector is the equal of the ideal detector of quantum efficiency of about 25%.

More intense pulses require the use of a larger number of output channels. We have tested our fiber-loop detector on different kinds of light pulses. The statistics has been artificially changed by changing the intensity of subsequent Poissonian pulses using a random number generator. The statistics  $P(I)$  of intensity fluctuations determines the true photon statistics of light pulses through the composition rule

$$\rho_n = \int \frac{I^n}{n!} e^{-I} P(I) dI. \quad (17)$$

Experimental results obtained with different light sources are summarized in Fig. 6. Notice that the composite nature of  $\rho$  nicely shows in the upper right panel. Also the super-Poissonian character of the input pulse is clearly seen in the lower left panel. Several tens of thousands of pulses were used for each reconstruction.

In conclusion we have demonstrated the photon-counting capability of the fiber-loop detector and quantified its efficiency by means of the Fisher information. The possibility to reconstruct the statistics of the input light pulses of moderate intensities have also been shown.

This work was partially supported by grants LN00A015, and RN19972003012 of the Czech Ministry

of Education, and by Czech-Italian project No. 29, “Decoherence and Quantum Measurement.”

---

- [1] J. Kim, S. Takeuchi, Y. Yamamoto, and H. H. Hogue, *Appl. Phys. Lett.* **74**, 902 (1999).
- [2] C. Kurtsiefer, S. Mayer, P. Zarda, and H. Wienfurter, *Phys. Rev. Lett.* **85**, 290 (2000).
- [3] S. Brattke, B. T. H. Varcoe, and H. Walther, *Phys. Rev. Lett.* **86**, 3534 (2001).
- [4] C. Santori, M. Pelton, G. Solomon, Y. Dale, and Y. Yamamoto, *Phys. Rev. Lett.* **86**, 1502 (2001).
- [5] M. Pelton, C. Santori, J. Vukovic, B. Zhang, G. S. Solomon, J. Plant, and Y. Yamamoto, *Phys. Rev. Lett.* **89**, 233602 (2002).
- [6] R. M. Stevenson, R. M. Thompson, A. J. Shields, I. Farrer, B. E. Kardynal, D. A. Ritchie, and M. Pepper, *Phys. Rev. B* **66**, 081302(R) (2002).
- [7] H. Paul, P. Törma, T. Kiss, and I. Jex, *Phys. Rev. Lett.* **76**, 2464 (1996).
- [8] P. Kok and S. L. Braunstein, *Phys. Rev. A* **63**, 033812 (2001).
- [9] K. Banaszek and I. A. Walmsley, *Optics Lett.* **28**, 52 (2003).
- [10] O. Haderka, M. Hamar, and J. Peřina Jr., [quant-ph/0302154](https://arxiv.org/abs/quant-ph/0302154).
- [11] S. L. Braunstein and K. Nemoto, *Phys. Rev. A* **66**, 032306 (2002).
- [12] C. R. Rao, *Bull. Calcutta Math. Soc.* **37**, 81 (1945).
- [13] H. Cramér, *Mathematical Methods of Statistics* (Princeton University Press, Princeton, NJ, 1946).
- [14] D. Mogilevtsev, *Opt. Communication* **156**, 307 (1998).
- [15] A. P. Dempster, N. M. Laird, , and D. B. Rubin, *J. R. Statist. Soc. B* **39**, 1 (1977).
- [16] Y. Vardi and D. Lee, *J. R. Statist. Soc. B* **55**, 569 (1993).